

# Field Measurement of Wayside Low-Frequency Noise Emitted from Tunnel Portals and Trains of High-Speed Railway \*

**K. Kikuchi<sup>1,2</sup>, M. Lida,<sup>1</sup> T. Takasaki<sup>1</sup> and H. Takami<sup>1</sup>**

*Environmental Engineering Division, Railway Technical Research Institute, 2-8-38, Hikari-cho, Kokubunji-shi, Tokyo, Japan, 185-8540 kikuchi@rtri.or.jp*

In order to determine the actual circumstances of wayside low-frequency noise and infrasound generated by high-speed trains (Shinkansen), field measurements were performed at two sites, one near a tunnel portal and the other in a fully opened section. The measurements were based upon the manual issued by the Ministry of the Environment of Japan in October 2000 and conducted to obtain G-weighted SPL, 1/3-octave band spectra, velocity dependence and distance attenuation of SPL. The measured results show that major components of the low-frequency noise from the tunnel portal are impulsive micro-pressure waves and continuous pressure waves, while those in the open section are near-field hydrodynamic pressure variations and far-field acoustic pressure waves.

## 1. INTRODUCTION

It cannot be said that low-frequency noise is fully understood. Its effects are sometimes confused with those of ground vibration, and the cause of indisposition is sometimes attributed to irrelevant low-frequency noise<sup>(1)</sup>. However, as public concerns about the effects of low-frequency noise had increased, the Ministry of the Environment of Japan (MOE) issued in October 2000 “Manual for measuring low-frequency noise<sup>(2)</sup>”, which was the first official document specifying the method of measuring low-frequency noise in Japan.

In the manual, high-speed railways (called “Shinkansen” in Japan) are given as an example of the sources of environmentally influential low-frequency noise. Although some measurements of low-frequency noise of Shinkansen obtained based upon the MOE manual have been reported, proper understanding of the phenomena has been insufficient. This paper presents the results of the measurement of way-side low-frequency noise generated by Shinkansen performed at two sites, one near a tunnel

portal and the other in a fully open air section. The measurement method for the low-frequency noise was based upon the MOE manual. The measured quantities were G-weighted SPL and 1/3-octave band spectra of the low-frequency noise in the range of 1 - 100 Hz (infrasound and low-frequency sound).

## 2. LOW-FREQUENCY NOISE EMITTED FROM TUNNEL PORTALS

When a train enters a tunnel at high speed, a compression wave is generated inside the tunnel. The compression wave propagates through the tunnel at the speed of sound, arrives at the exit portal and is reflected back as an expansion wave. Since a part of energy in the compression wave is emitted toward the outside of the tunnel, an impulsive low-frequency noise is observed near the tunnel portal (Fig. 1).

This phenomenon is called a “micro-pressure wave<sup>(3)-(6)</sup>,” which constitutes one of the typical wayside environmental problems of Shinkansen.

\*Reprinted with kind permission from the Journal of Low Frequency Noise, Vibration & Active Control

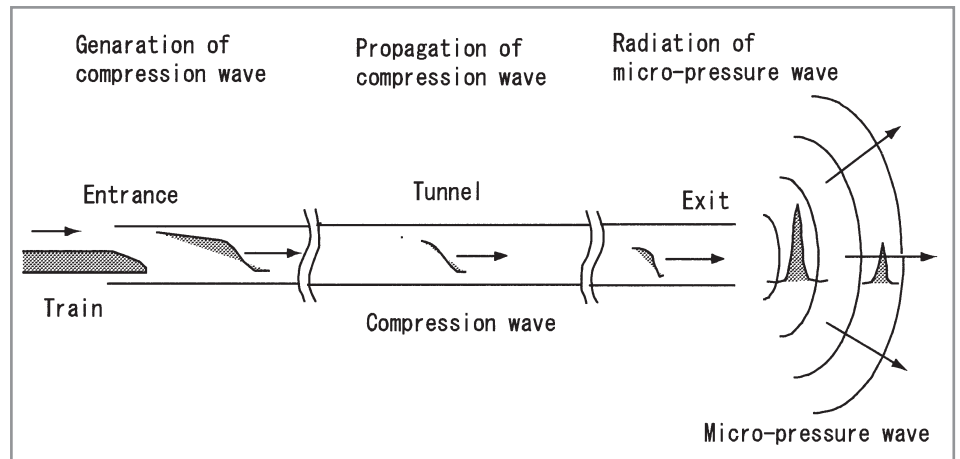


Figure 1. Generation of micro-pressure wave

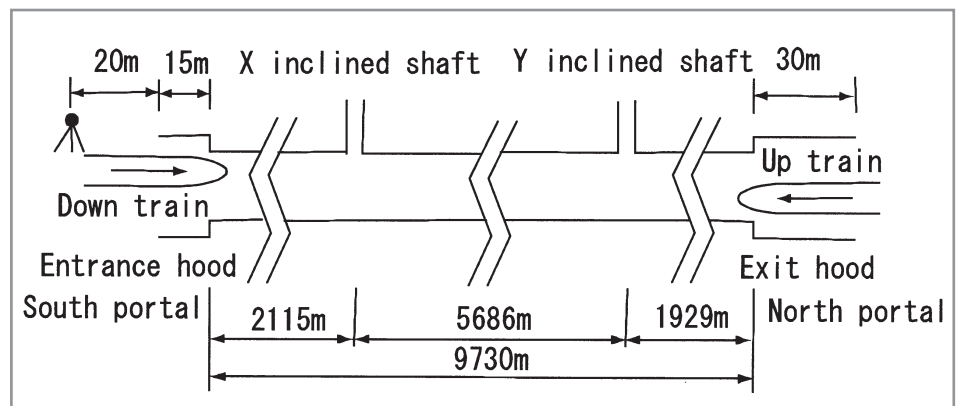


Figure 2. Outline of the measurement

After the micro-pressure wave radiation, pressure waves of relatively small amplitude continue to be emitted from the exit portal until the train leaves the tunnel. These continuous waves are considered to be generated by unsteady pressure variations around the train running inside the tunnel and we hereafter call them “continuous pressure waves<sup>(7)</sup>”. The continuous pressure waves are emitted not only from the exit portal but also from the entrance portal just after the train enters the tunnel.

## 2.1 OUTLINE OF MEASUREMENT

Figure 2 shows an outline of the measurement. The measured tunnel is 9730 m long and has a slab track (non-ballasted concrete track). A 15 m long hood is installed at the south end portal and a 30 m long hood is installed at the north end portal. The hoods have

openings on their side walls and they reduce the micro-pressure waves at the opposite portal by decreasing the pressure gradient of the compression wave generated during the entry of the train nose into the hood. The measurement point was located at 20 mm from the entrance plane of the hood installed at the south portal. Low-frequency noise was measured with a Rion NA-18A low-frequency sound pressure level meter<sup>(8)</sup>. Based on the MOE manual, measured data were recorded as time histories of G-weighted SPL and 1/3-octave band filtered SPL, from which we were able to obtain the peak values of G-weighted SPL and 1/3-octave band SPL (spectrum). The time constant in integration for sound pressure level is 1s (SLOW). Table I shows the specifications of measured Shinkansen trains.

Table 1. Specifications of trains

Train	Max. velocity (km/h)	Cross-sectional area (m <sup>2</sup> )	Nose length (m)	Train length (m)	Blockage of train to tunnel*
A	240	12.2	5.5	300, 12 cars	0.192
Up: B+C	275	B:11.2	B:8.9	B:200, 8 cars	B:0.177
Down: C+B		C:10.3	C:6.0	C:120, 6 cars	C:0.162
D	240	14.1	11.5	200, 8 cars	0.222

\*Cross-sectional area of a tunnel is 63.4m<sup>2</sup>

## 2.2 RESULTS

### 2.2.1 Time histories of SPL

Figure 3 shows two cases of measured time histories of G-weighted SPL one for up-train running from the north to the south portal and the other for down-train from the south to the north portal. SPL data for the up-train are shown from the instant of radiation of the micro-pressure wave by the train entry into the north portal to that of the train exit from the south portal. And SPL data for the down-train are shown from the instant of the train entry into the south portal to that of radiation of the micro-pressure wave by the train exit from the north portal. (When a train exits a tunnel, another compression wave is also generated in the tunnel, propagates backward inside the tunnel and radiates an impulsive pressure wave at the portal which the train entered from the open air section. This is also a micro-pressure wave and designated as “micro-pressure wave by train exit.”) Figure 3 shows both the G-weighted and the F-weighted (non-weighted, flat in 1 - 100 Hz) SPL data for comparison.

The sharp rise of SPL at about 25 s in the left figure for the up-train corresponds to the radiation of the micro-pressure wave. After the peak, the SPL falls less sharply, resulting in a saw-toothed shape. This is because the time constant for NA-18A is set at 1 s (SLOW). The low-frequency noise is generated continuously even after the radiation of the micro-pressure wave, because the continuous pressure wave is produced by the train running in the tunnel. The SPL of the continuous

pressure wave gradually increases as the train approaches the south portal. We can also see two distinct pressure waves at about 50 s and 105 s, which were generated by the train passage by the inclined shafts located at two midway points in the tunnel. This paper does not deal with these waves.

The right figure for the down-train shows a remarkably different pattern of SPL variation with time compared with the up-train. The first and second peaks observed at about 5 s corresponds to the near field pressure variations due to the passing of the nose and tail of the train in front of the measuring point, which will be described in detail in the section 3. After these peaks, continuous pressure waves are observed, but their SPL gradually decreases as the train goes away from the south portal. After the micro-pressure wave is emitted by the train exit from the north portal, which is the final peak of SPL at about 170 s, radiation of the low-frequency noise virtually stops and only breathing winds remaining inside the tunnel can be observed.

Figure 3 shows that there is a difference between the time histories of micro-pressure waves at train entry (much smoother) and that at train exit (much more irregular). The difference is thought to be caused by following reasons. The micro-pressure wave amplitude depends on the shape of the incident wave at the tunnel exit. When the wave front is steeper, the micro-pressure wave becomes larger. A compression wave which is generated at the nose of a train entering into a tunnel becomes significant in tunnels with

non-ballasted, modern concrete slab tracks, because nonlinear effects can cause the wave-front of the compression wave to steepen during its propagation along the tunnel. The magnitude of the micro-pressure wave generated by nose entry becomes large. Meanwhile, an expansion pressure wave which is generated at the tail of the train entering into a tunnel does not become significant in tunnels by nonlinear effects and the magnitude of micro-pressure wave by tail entry does not become so big. If these micro-pressure waves are compared, the micro-pressure wave at nose entry shows a larger value overwhelmingly. When the pressure fluctuation in such a situation is measured, a comparatively smoother time history in which only the micro-pressure wave by the nose entry appears is acquired. On the other hand, the nonlinear effects of propagation on the compression wave by the nose exit and on the expansion wave by the tail exit are small. The magnitudes of the micro-pressure waves by each pressure wave are the same degree respectively. When the pressure fluctuation in such a situation is measured, comparatively more irregular time histories in which both micro-pressure waves by the nose exit and those by the tail exit appear are acquired.

We also see there is a difference between the time histories of

continuous waves displayed in Figure 3a and those in Figure 3b. The time history the continuous wave in the case where the train approaches the measurement point is much smoother and that of the continuous wave in the case where the train leaves the measurement point is much more irregular.

We also see there is a difference between the time histories of continuous waves displayed in Figure 3a and those in figure 3b. The time history of the continuous wave in the case where the train approaches the measurement point is much smoother and that of the continuous wave in the case where the train leaves the measurement point is much more irregular. The reason of the difference is considered as follows. The frequency of the continuous wave in the case where the train approaches the measurement point is higher than that of the continuous wave in the case where the train leaves the measurement point because of the Doppler effect. When the waveform in the case where the train approaches the measurement is averaged over time constant 1s, it is thought that the comparatively smoother time history compared with the wave form in the case where the train leaves the measurement is recorded. We think further research on this point should be continued.

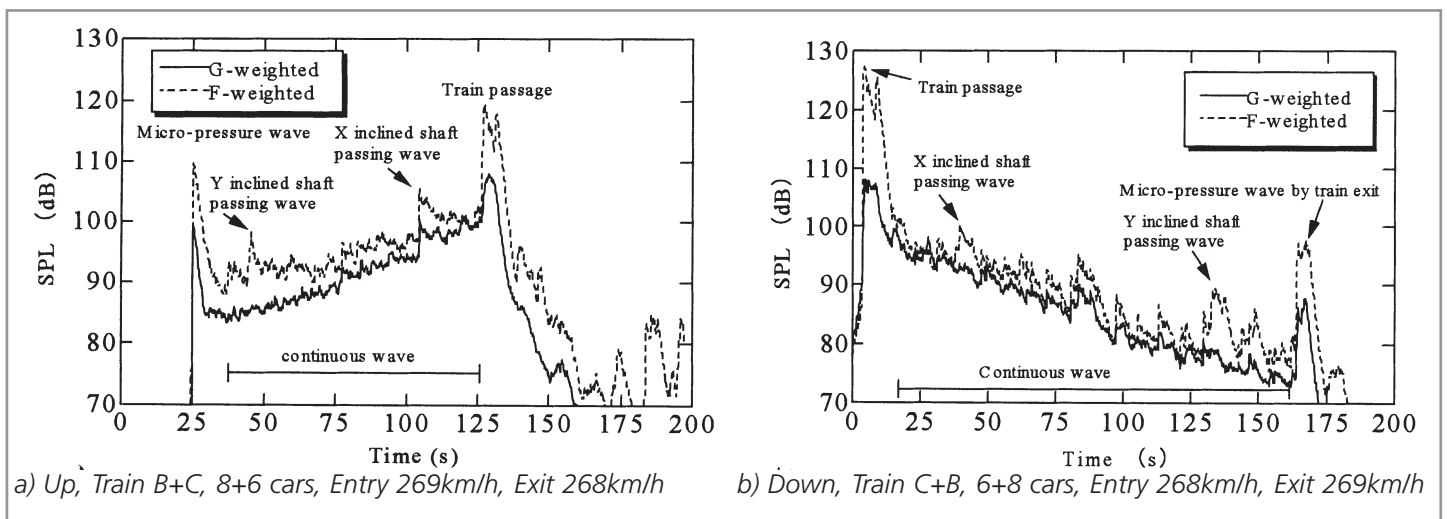


Figure 3. Sound pressure level observed at a tunnel portal

### 2.2.2 1/3-octave band SPL

Figure 4 shows an example of the measured 1/3-octave band SPL for the micro-pressure wave by the up-train. The SPL of each band in Figure 4 is the maximum value measured during the first few seconds corresponding to the micro-pressure wave radiation. Because the times when different 1/3-octave band SPLs take the maximum do not necessarily coincide with each other, we cannot regard Figure 4 as an instantaneous spectrum. For comparison, we show the curves of “threshold of rattling of windows, doors, etc.<sup>(9)</sup>”, and “threshold of feeling of pressure of vibration<sup>(10)</sup>”. From Figure 4, we can see that the main components of the micro-pressure wave are those having frequencies below about 10 Hz and the components having frequencies above about 10 Hz decrease as the frequency increases. The characteristic frequency of the micro-pressure wave is attributed to the train nose passage which is related to  $D/U$  where  $D$  is a tunnel radius or a train nose length and  $U$  is a train speed. In

this measurement, the characteristic length  $D$  is about several meters so the characteristic frequency becomes about 10 Hz. The reason why the frequency component above 10 Hz decrease largely is considered to be due to side branch effects. Side branches are usually arranged at regular intervals in long Shinkansen tunnels to install electrical equipment. Side branches have the effect of reducing the pressure gradient of the compression wave<sup>(3),(11)</sup>.

Figure 5 shows an example of measured 1/3-octave band SPL for the continuous pressure waves by the up- and down-trains. The SPL of each band in Figure 5 is the maximum value measured during the period from the instant just after the train entry to that just before the train exit. We cannot regard Figure 5 as an instantaneous spectrum in this case, either. The spectra of the continuous pressure waves do not include tonal components and exhibit a flatter distribution over the frequency range of 1 - 100 Hz than that of the micro-pressure wave.

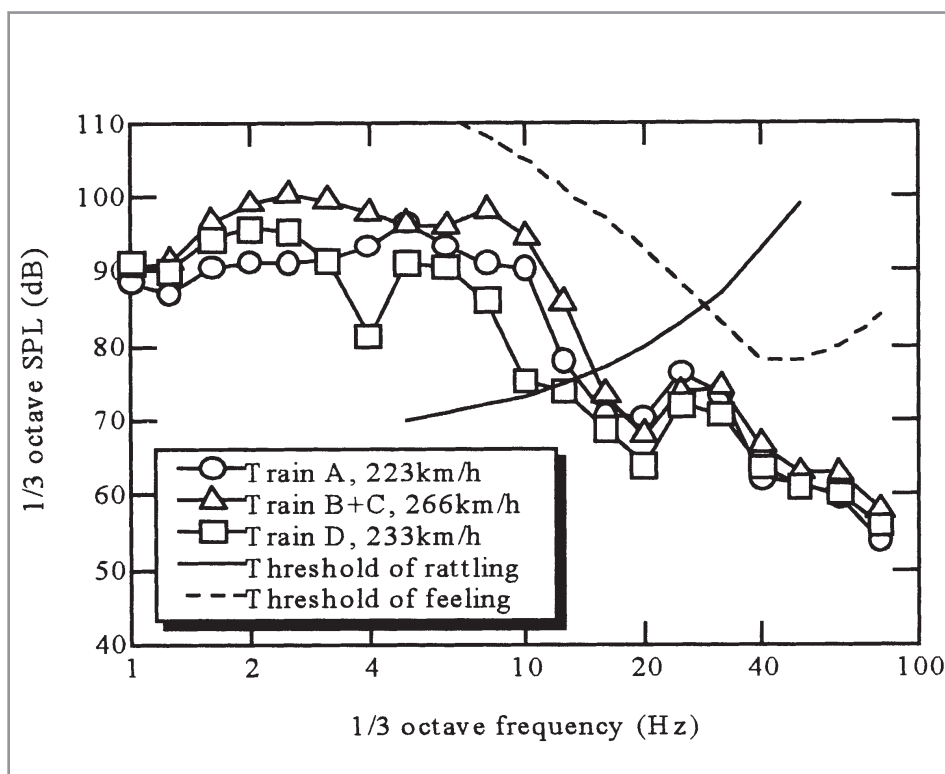


Figure 4. Spectra of 1/3 octave band SPL of micro-pressure wave

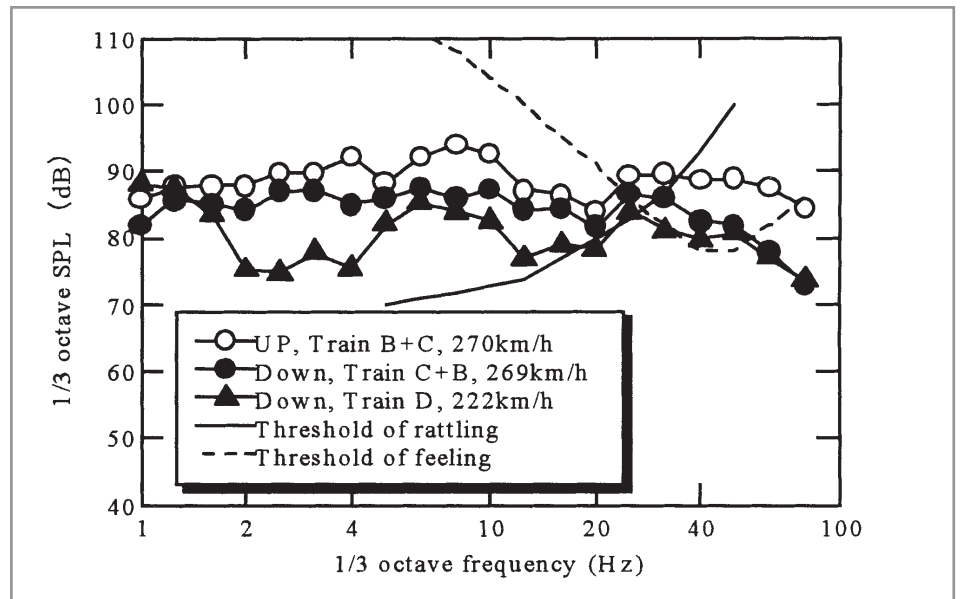


Figure 5. Spectra of 1/3 octave band SPL of continuous wave

### 2.2.3 Velocity dependency of G-weighted SPL

Figure 6 shows the velocity dependency of the maximum value of the G-weighted SPL for the micro-pressure wave by the up-train. The solid line designates the  $U^6$  law, where  $U$  is the speed of the up-train at the time of entry into the north portal. The  $U^6$  law holds for the maximum value of F-weighted SPL if we can neglect the effect of the

steepening of compression wave front by nonlinear propagation or that of flattening and attenuation of the compression wave by wall friction, ballast, side branches, etc. From Figure 6, we can at least say that the measured results do not contradict the  $U^6$  law although the speed range of each train is rather narrow to decide definite dependency.

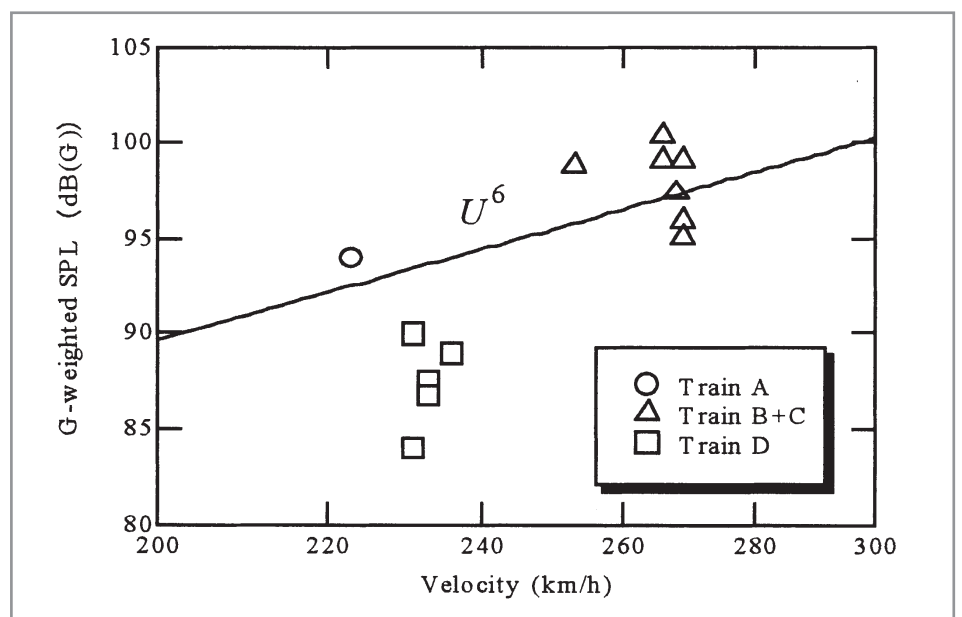


Figure 6. Relation between train velocity and peak value of G-weighted SPL of micro-pressure wave

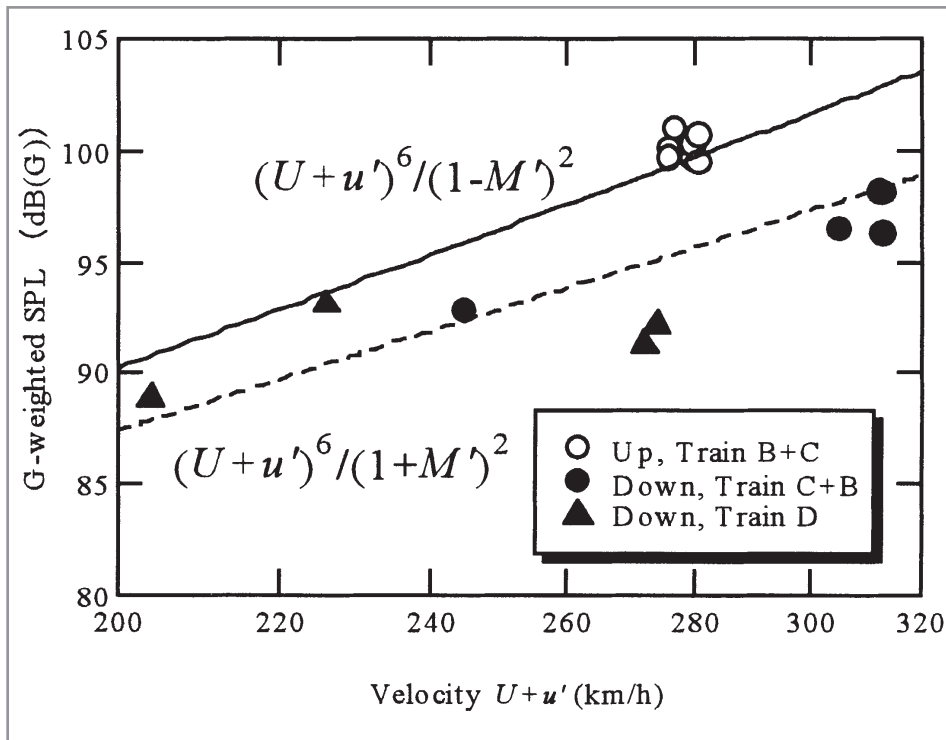


Figure 7. Relation between train velocity and peak value of G-weighted SPL of continuous wave

Figure 7 shows the velocity dependency of the maximum value of the G-weighted SOL for the continuous pressure waves by the up- and down-trains. As seen in Figure 3, SPL of the continuous pressure waves for the up-train becomes the maximum just before the train exits the tunnel and that for the down-train just after the train enters into the tunnel. We plotted these maximum values in Figure 7. The solid line and the dashed line designate  $(U + \dot{u})^6 / (1 - M')^2$  and  $(U + \dot{u})^6 / (1 + M')^2$ , respectively, where  $U$  is the train speed,  $\dot{u}$  is the speed of the air in the side region of train relative to the coordinate system fixed to the tunnel at the time when the continuous pressure becomes the maximum, and  $M' = (U + \dot{u}) / c_0$  ( $c_0$ : the speed of sound) is the Mach number of the speed  $U + \dot{u}$ . It was found from the past research<sup>(7)</sup> that the magnitude of the continuous pressure waves is related to the speed of the air in the side region of train relative to the coordinate system fixed to the train  $U + \dot{u}$ . We have calculated  $\dot{u}$  by using one dimensional analysis results<sup>(12),(13)</sup>.

From Figure 7, we can see that the G-weighted SPL for the continuous pressure waves is nearly proportional to the  $(U + \dot{u})^6$  law and the difference between the SPL for up-train and down-train is possibly explained by the effect of the Doppler factor,  $(1 + M')^2 / (1 - M')^2$ .

### 3. LOW-FREQUENCY NOISE EMITTED FROM TRAINS IN AN OPEN AIR SECTION

At a fixed point in an open air section, pressure variations are observed as a train nose or tail passes by. A simple mathematical model of this phenomenon is given by

$$p = \frac{1}{4\pi} \frac{q'[t - (R/c_0)]}{R(1 - M \cos \theta)^2} + \frac{q}{4\pi} \frac{(\cos \theta - M)U}{R^2(1 - M \cos \theta)^3} \quad (1)$$

where  $q$  is the source strength,  $q'$  is the time derivative of  $q$ ,  $U$  is the moving velocity,  $M(=U/c_0, c_0$  the speed of sound) is the Mach number,  $t$  is the time,  $R$  is the distance between the source and the observer,  $\theta$  is the angle between the direction of the velocity vector and that of the position vector of the observer relative to the source at the time of sound emission<sup>(14)</sup>. The first and second terms on the right and side of the Equation (1) represent an acoustic pressure wave and a hydrodynamic pressure variation (pseudo-sound) respectively. Since the second term decreases faster than the first term as the distance  $R$  increases, we can regard the first term as the far-field term and the second term as the near-field term. In general, the observer points, which can be considered to be the places where houses are located, exist not only in the far field but also in an intermediate region where the far-field and near-field terms are of the same order in magnitude.

Of course, the actual conditions of the low-frequency noise from the trains in an open air section are much more complex than what is represented by

Equation (1). However, it can still be said that the pressure variations due to the train passing consist of acoustic pressure waves and hydrodynamic pressure variations. Hereafter, we call the near-field hydrodynamic pressure variations<sup>(15),(16)</sup> “pressure variations due to train passing” and the far-field acoustic waves “low-frequency pressure waves” according to the conventional terminology.

### 3.1 OUTLINE OF MEASUREMENT

Measurement was performed along a viaduct of Shinkansen. Figure 8 shows an outline of the measurement. The viaduct is about 7 m high, with simple straight sound shield walls of 2 m height attached to both sides. The track alignment is straight and the track structure is a non-ballasted slab type. Three measurement points M1, M2 and M3 were located at 12.5m, 25 m and 50 m respectively from the center line of the viaduct. The measurement method of low-frequency noise is the same as that described in 2.1. Specifications of the measured Shinkansen trains are shown in Table II.

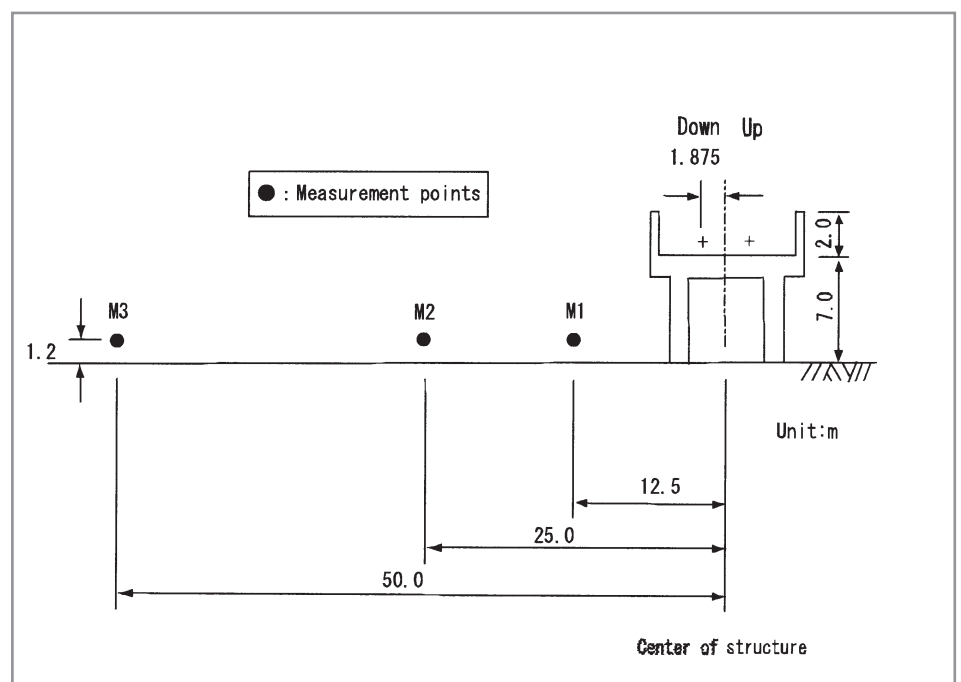


Figure 8. Schematic figure of field measurement

Table II. Specifications of trains

Train	Max. velocity (km/h)	Cross-sectional area (m <sup>2</sup> )	Nose length (m)
E	240	12.2	5.5
F	240	12.2	7.6
G	240	10.1	4.75
H	275	11.2	8.9
I	275 (340)	10.3	6.0
J	240	14.1	11.5

### 3.2 RESULTS

#### 3.2.1 Time histories of SPL

Figure 9 shows the time histories of G-weighted and F-weighted (flat in 1 - 100 Hz) SPL of the low-frequency noise measured at the points M1, M2 and M3 when a down-train of type H passed by at the speed of 246 km/h. The G-weighted SPL increases as the nose of the train approaches, keeps approximately constant while the intermediate part of the train is passing and decreases as the tail of the train goes away. While the F-weighted SPL exhibits two distinct peaks corresponding to the passing of the nose and tail, the G-weighted SPL shows only one gradual flat-top peak. This can

be understood in the following way. According to the previous researches, the near-field pressure variations due to the passage of the nose and tail mainly consist of frequency components approximately below 5 Hz and the far-field Acoustic pressure wave consists of frequency components approximately above 10 Hz. Hence, because the frequency characteristic of G-weighting has a peak at 20 Hz<sup>(17)</sup> and significantly decreases below 5 Hz, the near-field pressure variations due to the passage of the nose and tail have little contribution to the G-weighted SPL. Consequently the G-weighted SPL mainly depends on the low-frequency pressure waves.

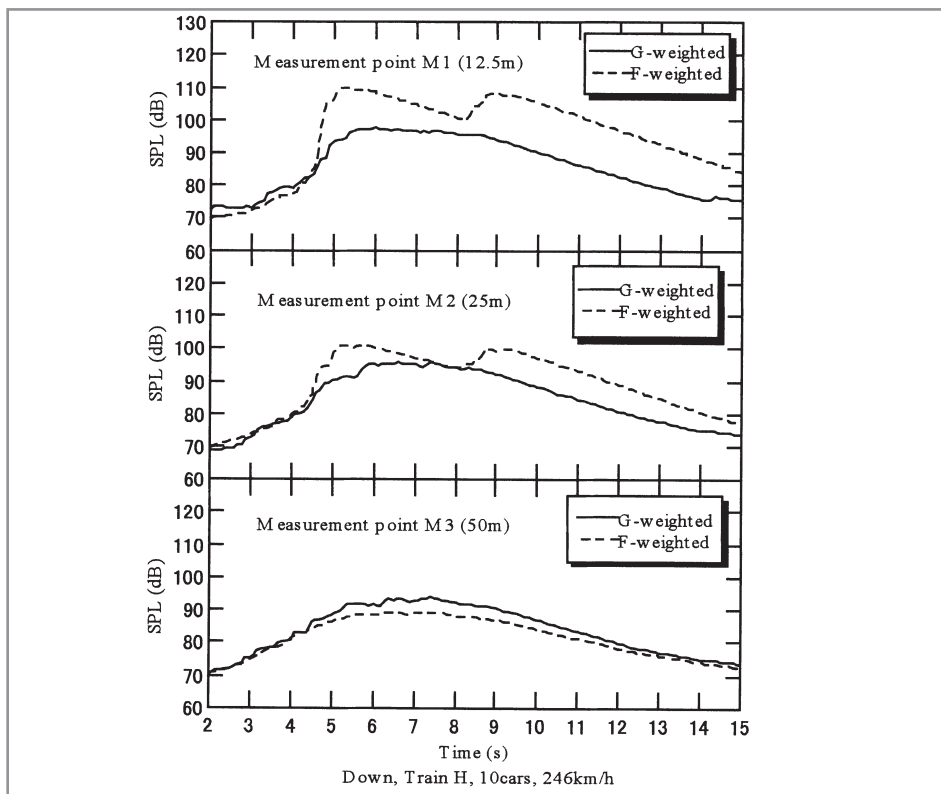


Figure 9. Time-history of G-weighted SPL measured at train passage

### 3.2.2 1/3 octave band SPL

Figure 10 shows an example of measured 1/3 octave band SPL for the low-frequency noise from the down-train of the train type I in an open air section. As in 2.2.2, the SPL of each band in Figure 10 is the maximum value measured during the passage of the train. From Figure 10 we can see that there is a trough at 2 - 8 Hz; 6 - 8 Hz at M1 (12.5 m point), 4 - 6 Hz at M2 (25 m point) and 2 - 3 Hz at M3 (50 m point). SPL decreases on the left side of this

trough as the frequency increases from 1 Hz and SPL increases on the right side as the frequency increases but remains roughly constant above 20 Hz. As mentioned above, the near-field pressure variations, mainly comprise components approximately below 5 Hz.

Consequently, we consider that the SPL on the left side of the trough corresponds to the near-field pressure variations and that on the right side corresponds to the far-field pressure waves.

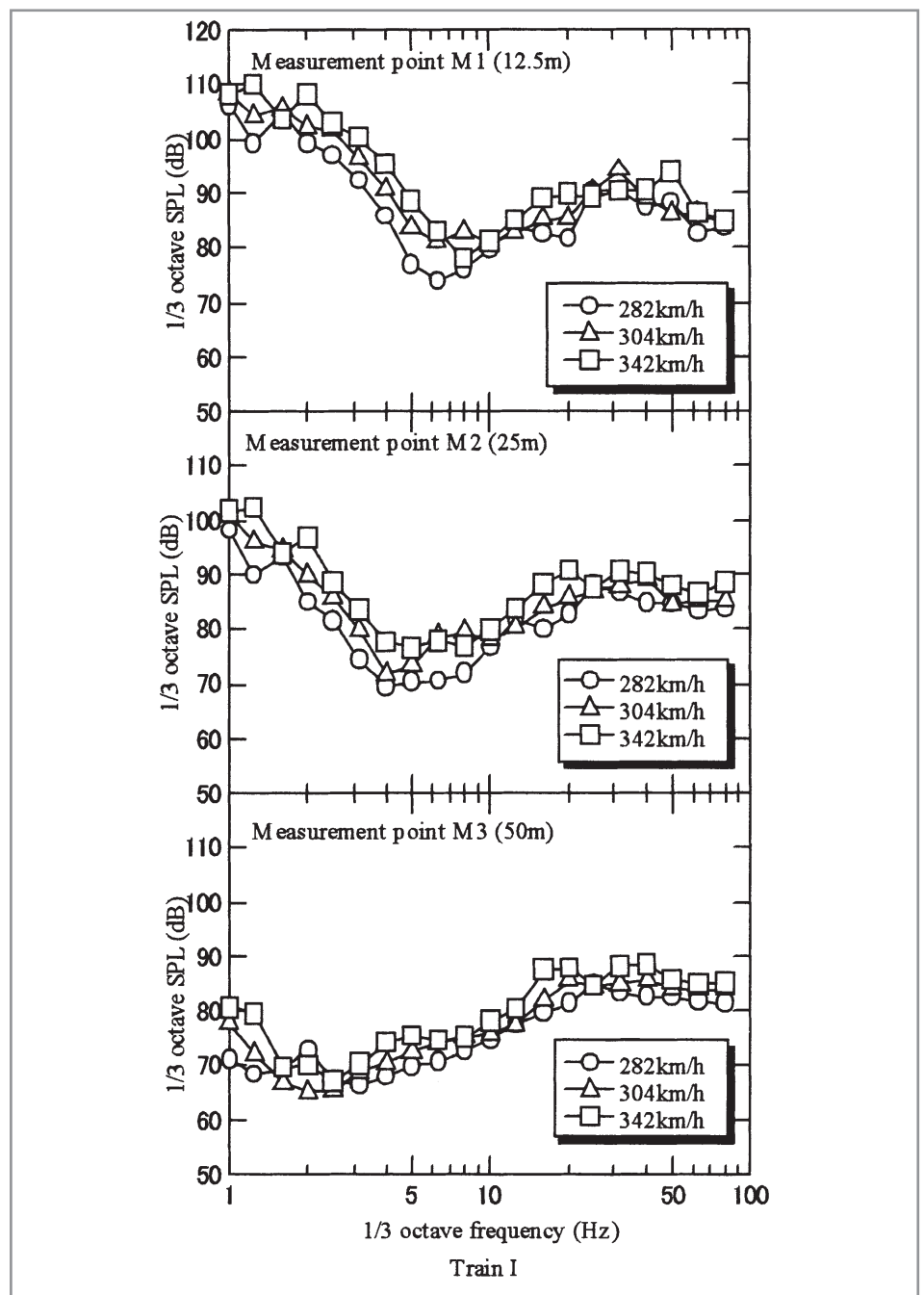


Figure 10. Spectra of 1/3 octave band SPL at train passage

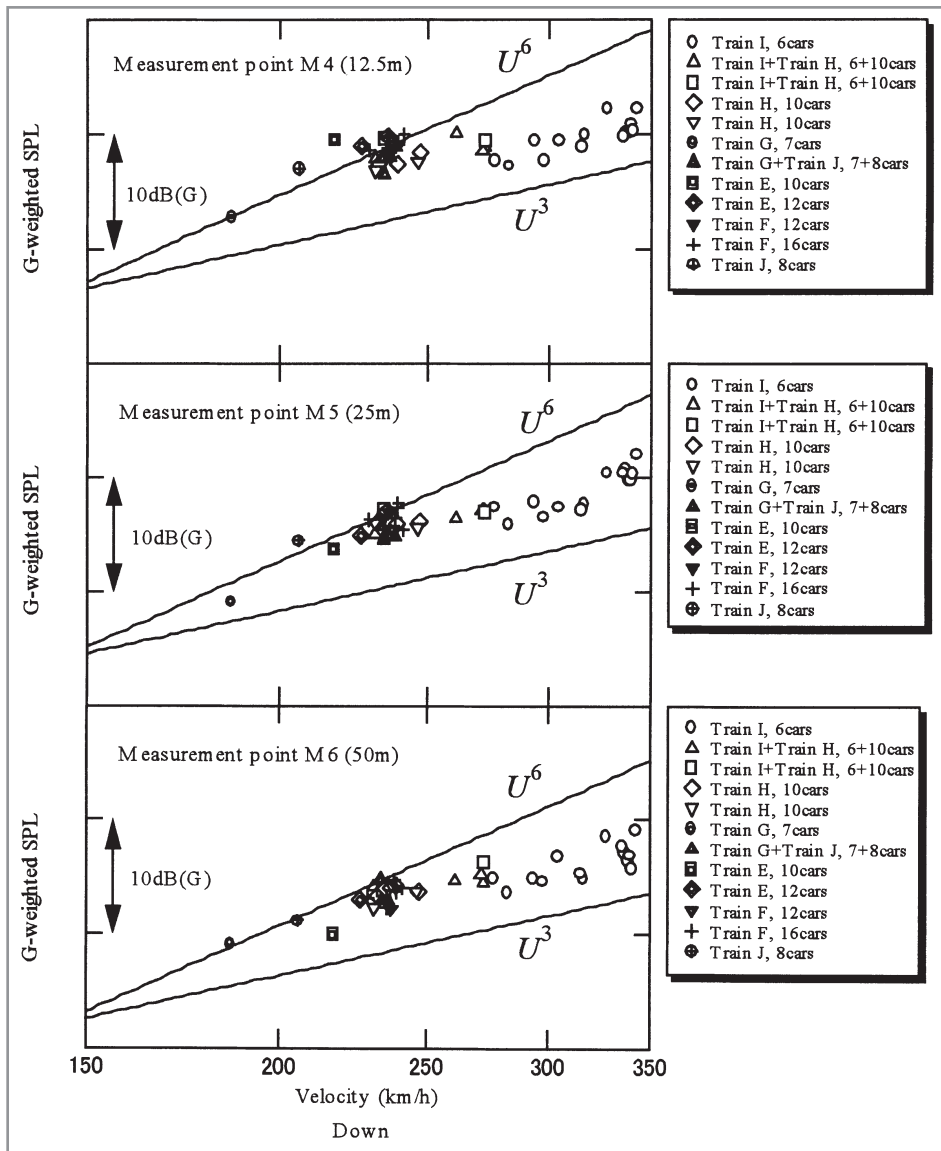


Figure 11. Relation between train velocity and peak value of G-weighted SPL

### 3.2.3 Velocity dependency of G-weighted SPL

Figure 11 shows the velocity dependency of the maximum value of the G-weighted SPL for the low-frequency noise in an open air section. The solid lines designate the  $U^3$  law and the  $U^6$  law, where  $U$  is the train speed. The  $U^3$  law can be applied to rolling noise and structural vibration noise<sup>(18)</sup>, while the  $U^6$  law to aeroacoustic noise<sup>(19)</sup>. The magnitude of G-weighted SPL depends on train types. The velocity dependency of the G-weighted SPL was calculated by using the data of train type I (its symbol is circle) which ran over the comparatively wide speed range.

From Figure 11, the velocity dependency of the G-weighted SPL is represented by the  $U^4 - U^5$  law. As stated in 3.2.1, the low-frequency pressure waves dominate the G-weighted SPL. Therefore we can say that the velocity dependency of the low-frequency pressure waves also follows the  $U^4 - U^5$  law. Based on only these results, however, we cannot decide which noise is the low-frequency pressure waves, structural vibratory noise or aeroacoustic noise (the scale of rails and wheels are so small that it is hard to believe that they are the sources of the low frequency pressure waves under 100 Hz).

### 3.2.4 Distance attenuation of G-weighted SPL

Figure 12 shows the distance attenuation of the maximum value of the G-weighted SPL for the low-frequency noise from down-trains of type H and type I. The broken lines designate the  $-10\log r$  law and the  $-20\log r$  law, where  $r$  is the distance between the center line of the viaduct and the measurement points. The  $-10\log r$  law holds if the acoustic source is a line source, while the  $-20\log r$  law holds if it is a point source. From Figure 12, the distance attenuation of the maximum of the G-weighted SPL coincides with the  $-10\log r$  law. Consequently, we can say that the G-weighted SPL depends on the acoustic low-frequency pressure waves, whose sources are classified as line sources.

## 4. CONCLUSIONS

Field measurements were performed on the wayside low-frequency noise of high-speed railways (Shinkansen) emitted from a tunnel portal and from a train in an open air section. The method was based upon the manual

issued by the Ministry of the Environment of Japan in October 2000. From the measured results, the following conclusions can be drawn.

### 4.1 TIME HISTORIES OF SPL

- Micro-pressure wave from a tunnel portal: The G-weighted SPL sharply rises at the arrival of the micro-pressure wave and thereafter falls gradually.
- Continuous pressure waves from a tunnel portal: The G-weighted SPL increases as the train approaches the portal from inside the tunnel and decreases as it goes away from the portal into the tunnel.
- Low-frequency noise in an open air section: The G-weighted SPL increases as the nose of the train approaches, keeps approximately constant while the intermediate part of the train is passing, and decreases as the tail of the train goes away. The G-weighted SPL in the open air mainly depends on the acoustic low-frequency pressure waves rather than the hydrodynamic pressure variations.

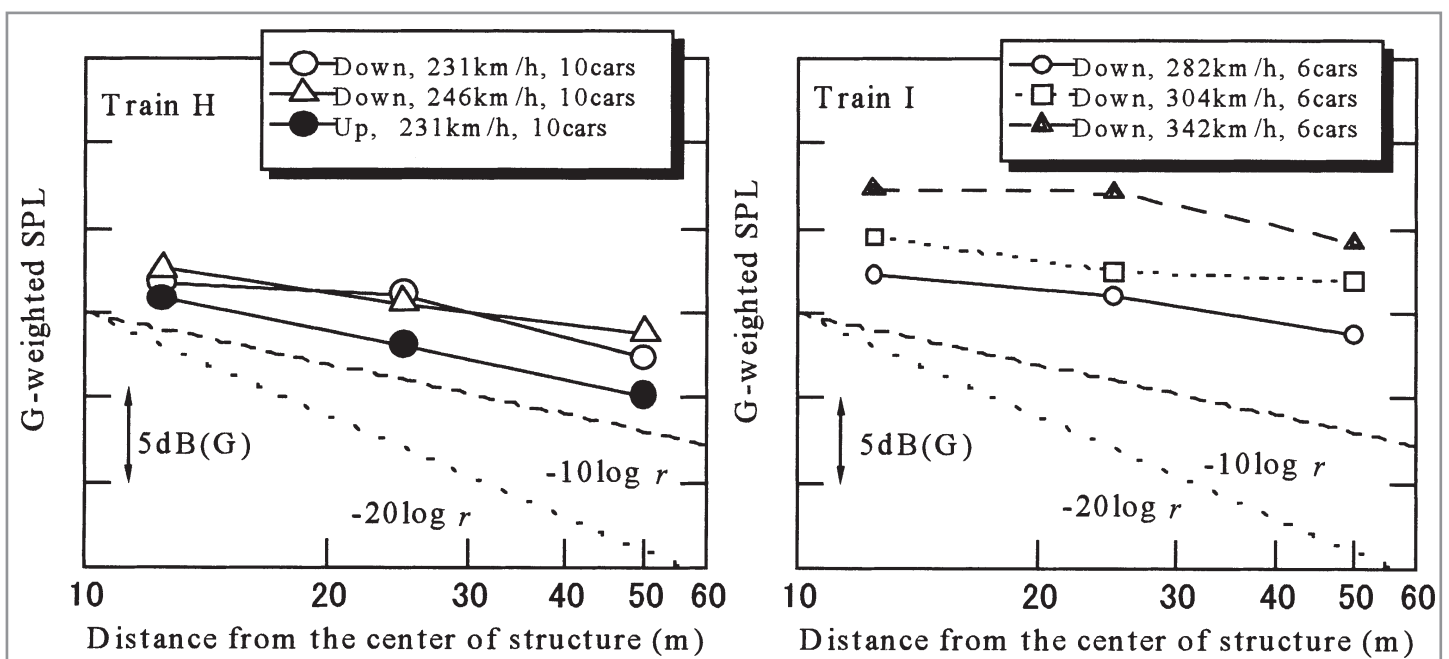


Figure 12. Relation between the distance from the center of structure and peak value of G-weighted pressure level

#### 4.2 1/3 OCTAVE BAND SPL

- Micro-pressure wave from a tunnel portal: The main frequency components of the micro-pressure waves are below 10 Hz.
- Continuous pressure waves from a tunnel portal: The spectra exhibit a comparatively flat distribution over the frequency range of 1 - 100 Hz.

#### 4.3 VELOCITY DEPENDENCY OF G-WEIGHTED SPL

- Micro-pressure wave from a tunnel portal: The G-weighted SPL is nearly proportional to the sixth power of the entry velocity.
- Continuous pressure waves from a tunnel portal: The G-weighted SPL is nearly proportional to the sixth power of the air velocity in train side region
- Low-frequency noise in an open air section: The G-weighted SPL is proportional to the fourth to fifth power of the running velocity.

#### ACKNOWLEDGEMENT

The authors wish to express their gratitude to Japan Railway companies for their great cooperation.

#### REFERENCES

(1) Geoff Leventhall, A. *Review of Published Research on Low Frequency Noise and its Effects*, Report for Defra, 2003

(2) The Ministry of the Environment of Japan. *Manual for measuring low-frequency noise*, 2000 (in Japanese)

(3) Satoru Ozawa, *Studies of micro-pressure wave radiated from a tunnel exit*, Railway technical research report, 1979 (in Japanese)

(4) Satoru Ozawa, et al., Countermeasures to reduce micro-pressure waves radiating from exits of Shinkansen tunnels, *Aerodynamics and Ventilation of Vehicle Tunnels*, 1991, pp. 253-266.

(5) R. Gregoire, et al., Experimental study (scale 1/70th) and numerical simulations of the

generation of pressure waves and micro-pressure waves due to high-speed train-tunnel entry, *BHR Group 1997 Vehicle Tunnels*, 1997, pp. 877-903

(6) M. S. Howe, The compression wave produced by a high-speed train entering a tunnel, *Proceedings of Royal Society of London*, A 454, 1998, pp.1523-1534

(7) Koji Nakatani, et al., Countermeasures to Reduce Low-Frequency Oscillation Generated by High Speed Shinkansen Train, *World congress on railway research proceedings*, Vol. E, 1997, pp. 491-497.

(8) Kiyokatsu Iwahashi, Hiroaki Ochiai, Infrasound Pressure Meter and Examples of Measuring Data, *Journal of Low Frequency Noise Vibration and Active Control*, Vol. 20 No. 1 (2001), PP.15-19

(9) Tokita et al., Proposal on the low frequency noise meter, *Proceedings of the conference on low frequency noise and hearing*, 1980, pp. 227-234

(10) Nakamura et al., Frequency characteristics of subjective response to low frequency sound, *Proceedings of Inter-noise 81*, 1981

(11) Lawrence E. Kinsler, et al., *Fundamentals of acoustics* Third edition, Wiley, 1982, pp. 234-242

(12) Tomoshige Hara, Aerodynamics drag of trains in tunnels, *Quarterly report RTRI*, Vol. 8, No. 4, 1967, pp. 229-235

(13) A E Vardy, Aerodynamic drag on trains in tunnels Part 2: *prediction and validation*, IMechE 1996, 1996, pp. 39-49

(14) P. M. Morse, K. U. Ingard, *Theoretical Acoustics*, Princeton University Press 1968, pp. 717-737

(15) Katsuhiko Kikuchi, et al., Numerical analysis of pressure validation under train passage using the boundary element method. *JSME International Journal*, Series B, Vol. 41, No. 3, 1998, pp. 624-631

#### THE BELGIAN APPROACH

The regional government of Wallonia is spending 438 million euros on anti-noise measures for the airports of Leige and Charleroi: acoustic insulation and purchase of houses. On 1 June 2005, 250 houses had been insulated, mainly in Liege. Works were proceeding in 290 others, among which 140 in Liege. The aim is to insulate 500 house by the end of 2005 and 1,200 per year from 2008.

#### MOTORCYCLES ATTACKED

Cities among favourite motorcycle routes concerned with the excessive bike noise, are beginning to crack down. In places like Laguna Beach, Calif., the Sunset Strip in West Hollywood and Main Street in Daytona Beach, Fla., police have set up patrols and decibel meters to enforce a more quiet ride, the Los Angeles Times reported. Some communities, including Myrtle Beach, S.C., are considering shortening, rescheduling or even doing away with motorcycle rallies. The industry has taken notice of the complaints as never before. In May, the 265,000-member American Motorcycle Association held its second "noise summit" in Columbus, Ohio, to tackle an issue it said represents the most pointed threat to bikers' rights.

- (16) T. Johnson, et al., 1/25 scale moving model tests for the TRANSAERO project, *TRANSAERO - A European initiative on transient aerodynamics for railway system optimisation*, Springer, 2002, pp. 123-135
- (17) ISO7196, *Acoustics-Frequency Weighting Characteristics for Infrasound Measurements*, (1995), pp. 1-6
- (18) E. K. Bender and P. J. Remington, The influence of rails on train noise, *Journal of Sound and Vibration*, Vol. 37, No. 3, 1974, pp. 321-334
- (19) N. Curle, The influence of solid boundaries upon aerodynamic sound, *Proceeding of Royal Society, A* 231, 1955, pp. 505-514

### **COLUMBUS UPDATES ORDINANCE**

Columbus is planning to create a clearer law to help cut down on excessive noise in the town. The town council is considering an updated ordinance that would give police officers a better tool for restricting noise. Columbus officer Andy Bennett proposed more detailed language for the ordinance so officers can clearly determine when there is a violation. As an example, he said the ordinance could state that a noise is too loud if it can be heard from 50 feet away in the day or 25 feet away at night. He said officers could issue a warning for the first offence and citations with escalating fines for subsequent offences. Bennett says he has a large folder for all the reports related to excessive noise within the past year. The town has had problems with loud car stereos and people playing music too late at night, he said: 'If I can hear it inside my house at 11 at night it's too loud,' he said. Councilman Tommy Melton said he thinks the town needs more "in depth" language in its noise ordinance. Bennett planned to develop a proposed update for the noise ordinance by pulling language from other municipal ordinances.

### **MOTORIZED TRICYCLES**

Fruit vendor Lucy Banquiao was shouting when she answered the interview about the noise and air pollution in this Philippine city of more than 100,000 people. She was also covering her mouth and nose to avoid inhaling the fumes coming from smoke belching vehicles. A recent study by the Department of Environment and Natural Resources found that the noise level in Pagadian City's commercial areas was above tolerable level and the air quality very unhealthy. In the study, the DENR identified three sampling sites, two commercial areas and one residential. In all three sites the average noise level is 80 decibels (dB) as found in the seven trials conducted. The survey's result showed that even in residential areas, the noise is above the standards of 55 dB and 65 dB during daytime in commercial areas. The DENR study attributed the noise and air pollution to "motor vehicles specifically the tricycles and motorcycles playing major routes of the city." Motorized tricycles, which number about 2,850 according to the city's business tax office, are the principal mode of transportation around the city. Dr Edgar Legazpi, environment committee chair of the Zamboanga del Sur Medical Society (ZSMS) said the noise generated by tricycles was due to the modification of the muffling system of the engines "The original engine is not noisy but because they wanted to load more passengers, they change the muffler so the tricycle can still run even though it is overloaded," said Legazpi. Elinor Egoogan, automotive specialist and instructor in one of the vocational schools here, said some operators changed the silencer of the motor engine to boost the power of the engine so that the tricycles could maneuver in upslope roads. He also attributed the noise and air pollution to old tricycles which are still allowed to ply in the city.